Skin effect and winding number in disordered non-Hermitian systems

Jahan Claes and Taylor L. Hughes

Phys. Rev. B **103**, L140201 — Published 6 April 2021

DOI: 10.1103/PhysRevB.103.L140201

Skin effect and winding number in disordered non-Hermitian systems

Jahan Claes and Taylor L. Hughes
Department of Physics and Institute for Condensed Matter Theory, University of Illinois at Urbana-Champaign, Illinois 61801, USA

Unlike their Hermitian counterparts, non-Hermitian (NH) systems may display an exponential sensitivity to boundary conditions and an extensive number of edge-localized states in systems with open boundaries, a phenomena dubbed the "non-Hermitian skin effect." The NH skin effect is one of the primary challenges to defining a topological theory of NH Hamiltonians, as the sensitivity to boundary conditions invalidates the traditional bulk-boundary correspondence. The NH skin effect has recently been connected to the winding number, a topological invariant unique to NH systems. In this paper, we extend the definition of the winding number to disordered NH systems by generalizing established results on disordered Hermitian topological insulators. Our real-space winding number is self-averaging, continuous as a function of the parameters in the problem, and remains quantized even in the presence of strong disorder. We verify that our real-space formula still predicts the NH skin effect, allowing for the possibility of predicting and observing the NH skin effect in strongly disordered NH systems. We use our theory to demonstrate the NH Anderson skin effect, in which a skin effect is developed as disorder is added to a clean system, as well as explain recent results in optical funnels.

INTRODUCTION

The topological classification of Hermitian Hamiltonians[1–8] applies to non-interacting Hamiltonians in equivalence classes based on the ten internal Altland-Zirnbauer (AZ) symmetry classes[9]. The topological classifications for these symmetry classes are known for all spatial dimensions, and explicit forms for the corresponding topological invariants have been constructed[4–8]. A notable feature of the Hermitian topological classification is the celebrated *bulk-boundary correspondence*, in which topological invariants of the bulk system predict anomalous states on the boundary[1–3].

There has been recent interest in the topological properties of non-Hermitian (NH) Hamiltonians[10–25]. NH Hamiltonians provide effective models for quantum systems with gain and loss[26], and can be realized in atomic[27–31], optical[22–25, 32–40], electronic[41–43] and mechanical[44–49] systems. Like their Hermitian counterparts, NH Hamiltonians can display protected anomalous boundary states[12, 13, 19]. In addition, they display topological phenomena unique to NH systems, such as exceptional points[19, 50], half-integer winding[19], stable 2D semimetallic phases[50–53], and Weyl exceptional rings[27, 37]. All of these phenomena are tied to a richer set of symmetry classes beyond the ten AZ classes[52–55].

A challenge for understanding the topological phenomena of NH Hamiltonians is the NH skin effect, in which systems may display remarkably different eigenspectra and eigenstates in periodic vs open boundary conditions (PBC or OBC) [16, 56–59]. In particular, PBC and OBC systems may become gapless at different points in their phase diagrams[16, 20, 58–60], topological invariants calculated using PBC may not predict properties of the OBC system, and topologically protected edge states in OBC systems may be hidden in an extensive number of edge-localized eigenstates. To determine topological properties of OBC systems, one may compute the so-called generalized Brillouin zone[16, 20, 60], which can be done only for simplified models, or by use real-space invariants that directly predict OBC properties[59, 61–63]. However, in general, a precise understanding of the NH skin effect is necessary to develop a bulk-boundary correspondence for NH systems[64]. The NH skin effect is also interesting in its own right, as systems with the NH skin effect exhibit exponentially large responses to perturbations[44, 47], and optical systems exhibiting the NH skin effect have recently been demonstrated to funnel light for high-performance optical sensors[40].

While understanding the NH skin effect and its relationship to the bulk-boundary correspondence is still an outstanding question in general dimensions, in 1D it has recently been shown that the NH skin effect is determined by the winding number around a complex energy E: $w(E)$[65–67]. The winding number is a topological invariant unique to NH systems[15, 52] and, roughly speaking, regions of the complex energy plane with nonzero $w(E)$ under PBC have dramatically different spectra and localization properties under OBC. Thus, determining $w(E)$ predicts the presence or absence of a NH skin effect in the neighborhood around E.

In this work, we generalize the winding number $w(E)$ to disordered NH systems. We accomplish this by mapping the the NH problem to a disordered Hermitian system, for which previous results have been established. We propose a real-space formula for $w(E)$ that is self-averaging, continuous as a function of the parameters in the problem, and remains quantized even in the presence of strong disorder. We verify the stability of our invariant in simple models of NH systems with nontrivial

winding. We also demonstrate that our invariant $w(E)$ determines the existence of the NH skin effect and, when non-vanishing, also predicts the existence of an entire band of delocalized states in our system. Indeed, the non-zero winding essentially protects these states from localization, in striking contrast to disordered 1D Hermitian systems which are always localized (unless tuned to a critical point)[68, 69]. Our work is distinct from previous work on topological properties of disordered NH systems [61–63], which studied the chiral winding ν rather than the NH winding $w(E)$.

The NH skin effect has already been observed in optical[39], electronic[41, 42], and mechanical[44–46] systems, so our results can be experimentally realized in multiple contexts. In addition, our results have positive implications for the stability of the recently demonstrated optical funnel[40] to disorder. Finally, since our method holds at arbitrary disorder strength, our results predict the possibility of observing a "NH Anderson skin effect," a NH analogue of the topological Anderson insulator[61, 63, 68–72], in which the skin effect is induced entirely by disorder from a clean system with no skin effect.

BACKGROUND: THE NH WINDING NUMBER AND THE SKIN EFFECT

As in the Hermitian case, the eigenstates of a translationally invariant NH Hamiltonian can be written via Bloch's theorem as $|\psi_k^n\rangle = e^{ik\hat{X}}|u_k^n\rangle$, with $\hat{H}|\psi_k^n\rangle = E_k^n|\psi_k^n\rangle$, $k \in [0, 2\pi]$. Unlike in the Hermitian case, the eigenvalues E_k^n can in general be complex. Fig. 1(a) illustrates possible curves E_k^n for a two band model. Because the spectrum is complex, we can distinguish two types of gaps. *Point gaps* are values $E \in \mathbb{C}$ such that the bands E_k^n never intersect E, while *line gaps* are lines $\ell \subset \mathbb{C}$ such that the bands never intersect ℓ[15, 54]. These gaps coincide for Hermitian systems, but are distinct for NH systems.

For any point gap E, we can define a topological invariant $w(E)$ that counts how many times the bands E_k^n wind around E. Note that $w(E)$ cannot change unless the gap closes at E. We can write a formula for the winding number[15]:

$$w(E) = \frac{1}{2\pi i}\int_0^{2\pi} \partial_k \log\left(|\hat{H}_k - E|\right)\, dk. \qquad (1)$$

This counts the number of times the determinant of $(\hat{H}_k - E)$ winds around the origin, which is equivalent to counting the total winding of the bands E_k^n around E. The winding numbers are indicated by the integers in Fig. 1(a).

It has recently been proven that $w(E)$ predicts the NH skin effect[65–67]. Concretely, when transitioning between PBC and OBC, the PBC eigenvalues enclosing a region with $w \neq 0$ collapse onto 1D arcs within the region. An example is shown in Fig. 1(b), where the OBC eigenvalues appear in the interior of the regions having $w = \pm 1$. Moreover Refs. [66, 67] proved that the OBC eigenvalues located in the interior of regions having $w > 0$ correspond to eigenstates localized at the right edge of the system, and the OBC eigenvalues located in the interior of regions where $w < 0$ correspond to eigenstates localized at the left edge of the system, as is shown in Fig. 1(c). The number of eigenvalues in each arc is proportional to the system size, leading to an extensive number of states at the corresponding edge. The marked difference between OBC and PBC spectra and the extensive number of edge states always occur together, and collectively make up the NH skin effect[16].

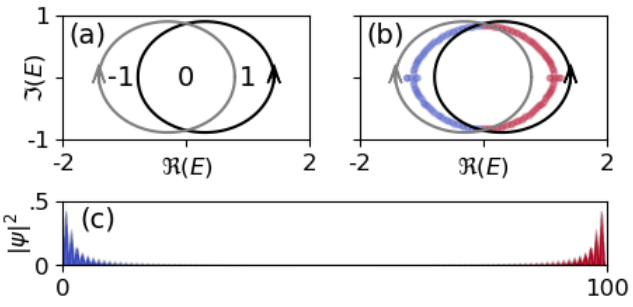

FIG. 1. An example of a NH band structure with +1 and −1 winding. (a) The PBC bands in the complex plane, with the winding numbers marked. (b) The same diagram, with the OBC spectrum overlaid. Red denotes states in a region with $w(E) > 0$, blue denotes states in a region with $w(E) < 0$. We see that the regions with positive/negative winding collapse onto lines. (c) The density $|\psi^n(x)|^2$ of all OBC eigenstates $\{\psi^n\}$. We see that eigenstates in regions with negative winding (blue) are localized at the left edge, while eigenstates in regions with positive winding (red) are localized at the right edge.

THE DISORDERED NH WINDING NUMBER

Ref. 15 previously introduced a formula for the winding number in the presence of disorder. Adding flux ϕ through the periodic system, they define the winding number by

$$w(E) = \frac{1}{2\pi i}\int_0^{2\pi} \partial_\phi \log\left(|\hat{H}(\phi) - E|\right)\, d\phi. \qquad (2)$$

This formula has been successfully applied to a NH version of the quasiperiodic Aubry-Andr-Harper model[73, 74] to predict topological localization transitions[75, 76], mobility edges[76], and the NH skin effect[43]. However, for models at strong disorder this formula has a few drawbacks. Most notably, it requires evaluating the integrand at many values of ϕ to estimate the integral. In addition, it is not clear that this formula is self-averaging for

large systems. Finally, it is not obvious that this formula is well-behaved at strong disorder when eigenvalues will exist near E so that the phase of $|\hat{H}(\phi) - E|$ is sensitive to rounding errors.

In this paper, we instead define a real-space formula for the winding number $w(E)$ using techniques from non-commutative geometry. Our formula relies on mapping a NH Hamiltonian $\hat{H}$ to a doubled Hermitian Hamiltonian $\hat{\mathcal{H}} = \hat{\sigma}_+ \otimes (\hat{H} - E) + \hat{\sigma}_- \otimes (H - E)^\dagger$ with chiral symmetry $\hat{S} = \hat{\sigma_z} \otimes \mathbb{1}$[15], and applying known results from non-commutative geometry to $\hat{\mathcal{H}}$ [68, 69, 77, 78]. Concretely, we define an operator $\hat{Q}$ by the polar decomposition $(\hat{H} - E) = \hat{Q}\hat{P}$, where $\hat{Q}$ is unitary and $\hat{P}$ is positive. Refs. 15 and 79 have previously used $\hat{Q}$ to define topological properties of clean NH systems. Given $\hat{Q}$, we define

$$w(E) = \mathcal{T}(\hat{Q}^\dagger[\hat{Q}, \hat{X}]), \tag{3}$$

where $\mathcal{T}$ is the trace per unit volume and $\hat{X}$ is the position operator. This reduces to Eq. 1 when the system is translationally invariant. In addition, $w(E)$ is quantized, self-averaging, continuous as a function of E and parameters in the Hamiltonian, and only changes when there are states with diverging localization length $\Lambda(E)$ at E. Furthermore, a semi-infinite system has an eigenstate with eigenvalue E localized at the boundary whenever $w(E) \neq 0$, which provides a justification of Eq. 3 as the real-space generalization of the winding number (see Supplement[80] for more details). Our formula for $w(E)$ is a real-space NH invariant in the spirit of Refs. 61–63, although unlike those works our invariant has no Hermitian counterpart.

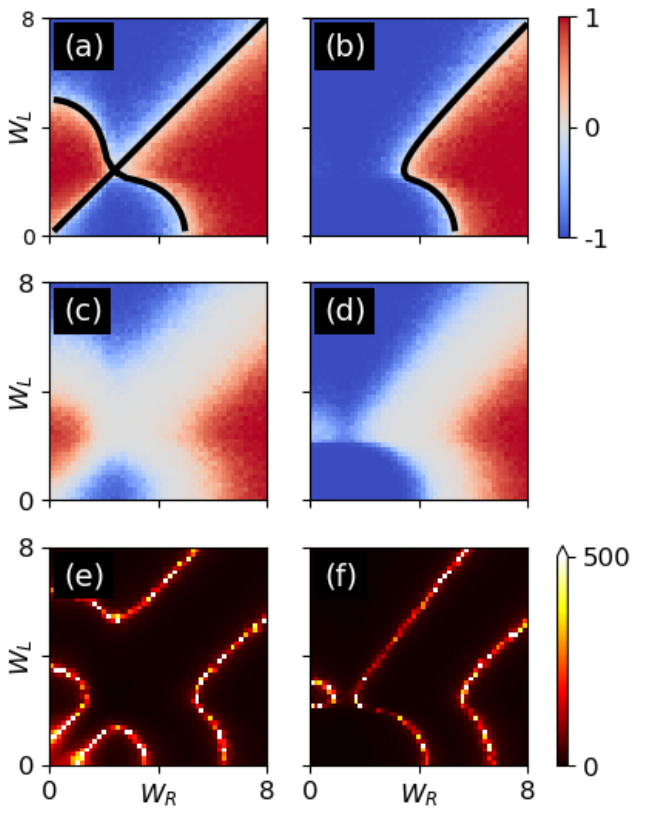

FIG. 2. (a) $w(0)$ as a function of (W_R, W_L) for $(J_L, J_R, W) = (1, 1, 0)$. The black line denotes the points where $\Lambda(0)$ diverges. (b) Same plot for $(J_L, J_R, W) = (1, .5, 0)$. (c,d) $w(E)$ as a function of (W_R, W_L) for $(J_L, J_R, W) = (1, 1, 1)$ and $(J_L, J_R, W) = (1, .5, 1)$. (e,f) Numerically computed $\Lambda(0)$. In all cases, $w(0)$ transitions when $\Lambda(0)$ diverges.

HATANO-NELSON MODEL WITH DISORDER

To illustrate the properties of $w(E)$, we consider the Hatano-Nelson model [81–83]:

$$\hat{H} = \sum_i J_R^i \hat{c}_{i+1}^\dagger \hat{c}_i + J_L^i \hat{c}_i^\dagger \hat{c}_{i+1} + h^i \hat{c}_i^\dagger \hat{c}_i. \tag{4}$$

This model describes a uniform chain with independent hoppings J_L^i and J_R^i in the left and right directions, and an on-site potential h^i (which we take to be real). This model is non-Hermitian when $J_L^i \neq J_R^i$. To model disorder we choose the hopping parameters via

$$J_R^i = J_R + W_R \omega_R^i, \quad J_L^i = J_L + W_L \omega_L^i, \quad h^i = W\omega^i, \tag{5}$$

where $\omega_{(L/R)}^i \in [-.5, .5]$ are uniformly distributed independent random variables.

We can illustrate the behavior of $w(E)$ in multiple ways. First, if we consider the winding only around $E = 0$ and set the onsite disorder $W = 0$, then we can use the method of Ref. 69 to analytically compute the localization length $\Lambda(0)$:

$$\frac{1}{\Lambda(0)} = \log\left(\frac{|J_R - \frac{W_R}{2}|^{\frac{J_R}{W_R} - \frac{1}{2}} |J_L + \frac{W_L}{2}|^{\frac{J_L}{W_L} + \frac{1}{2}}}{|J_R + \frac{W_R}{2}|^{\frac{J_R}{W_R} + \frac{1}{2}} |J_L - \frac{W_L}{2}|^{\frac{J_L}{W_L} - \frac{1}{2}}}\right). \tag{6}$$

In Figs. 2(a,b), we plot the numerically computed $w(0)$ and the analytically predicted curves where $\Lambda(0) = \infty$ as a function of the disorder parameters (W_L, W_R), at fixed model parameters (a) $(J_L, J_R, W) = (1, 1, 0)$ and (b) $(J_L, J_R, W) = (1, .5, 0)$. We find $w(0)$ is quantized, and only changes when $\Lambda(0)$ diverges. At more general E and/or nonzero W, we cannot analytically determine the phase boundaries. However, for a general (J_R, J_L, W) and general E, we can compute $\Lambda(E)$ numerically using transfer matrices[84]. In Figs. 2(c-f), we plot $w(0)$ and $\Lambda(0)$ for systems with (c,e) $(J_L, J_R, W) = (1, 1, 1)$ and (d,f) $(J_L, J_R, W) = (1, .5, 1)$. We again find $w(E)$ is quantized and transitions only when $\Lambda(E)$ diverges.

To illustrate the localization properties of the spectrum we consider a system at fixed disorder, and calculate $w(E)$ as a function of E. If we assume $(W_L, W_R) = 0$ and let h^i follow a Cauchy distribution rather than a

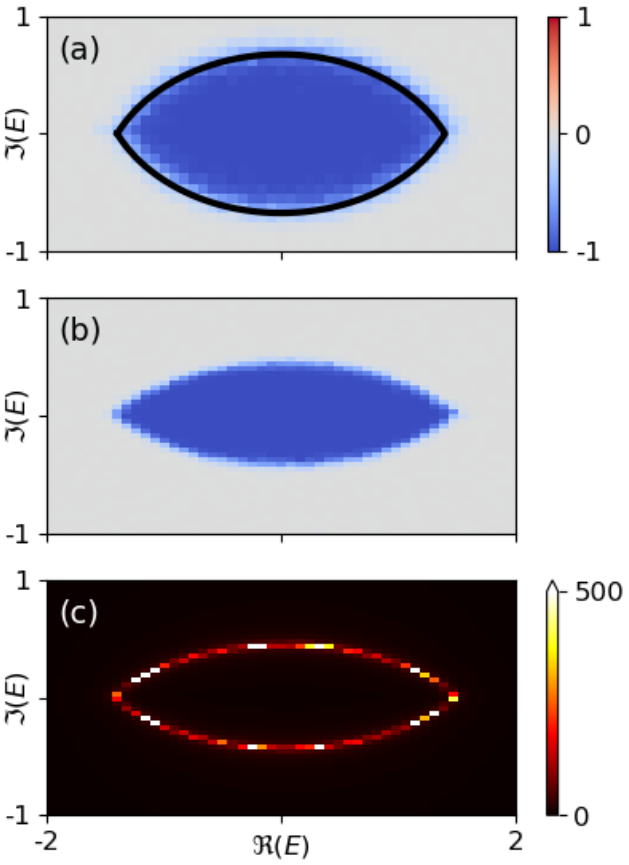

FIG. 3. (a) $w(E)$ for a system with $W_L = W_R = 0$ and h^i distributed according to a Cauchy distribution. The black line denotes the values where $\Lambda(E)$ diverges. (b) $w(E)$ for a system with $(J_L, J_R, W_L, W_R, W) = (1, .5, 1, 1, 1)$. (c) Numerically computed $\lambda(E)$. In each case, the region with $w(E) \neq 0$ is surrounded by a wall of delocalized states, and $w(E)$ only transitions when $\Lambda(E)$ diverges.

uniform distribution, we can compute $\Lambda(E)$ analytically at any E[85, 86]; this is shown in Fig. 3(a). For more general disorder, we can again use the transfer matrix; an example with $(J_L, J_R, W_L, W_R, W) = (1, .5, 1, 1, 1)$ is shown in Fig. 3(b,c). In both cases, a region with nonvanishing winding is completely surrounded by delocalized states. These examples reveal a notable distinction between the NH winding number $w(E)$ and Hermitian topological invariants such as the chiral winding number ν and the Chern number C. Indeed, ν is a stable topological invariant that is carried by entirely localized states[69], while the Chern number can be carried by a single delocalized state[87–89]. The NH winding, by contrast, can be nonzero only when an extensive number of delocalized states exist in the spectrum. This is because $w(E)$ only changes when E passes through a delocalized state, and $w(E) \to 0$ as $|E| \to \infty$ since in this limit $\hat{Q}$ approaches the identity matrix. This implies that any E with a nonzero winding must be surrounded by a "wall"

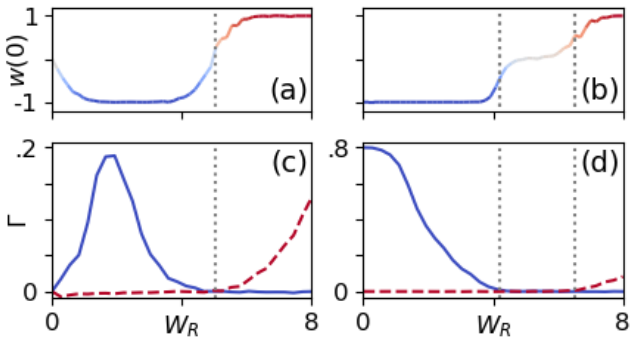

FIG. 4. (a) $w(0)$ as a function of W_R for $(J_L, J_R, W, W_L) = (1, 1, 0, 0)$. This corresponds to the x-axis in Fig. 2(a). (b) The same for $(J_L, J_R, W, W_L) = (1, .5, 1, 0)$, corresponding to the x-axis in Fig. 2(e). (c,d) The corresponding slopes Γ in the relation $\rho_{\text{edge}} = \Gamma N$ for the left (blue solid) and right (red dashed) edges. We see that the NH skin effect occurs at the left edge when $w < 0$ and at the right edge when $w > 0$.

of delocalized states, and the nonzero winding prevents these states from localizing. Intuitively, an extensive sensitivity to boundary conditions should require an extensive number of delocalized states, and this is precisely what we find.

$w(E)$ AND THE NH SKIN EFFECT

In clean systems, a region having winding $w > 0$ leads to an extensive number of states at the right edge of the system, and a region having winding $w < 0$ leads to an extensive number of states at the left edge of the system[66, 67]. We can characterize this NH skin effect by examining the density $\sum_n |\psi^n(x)|^2$ of all modes $\{\psi^n\}$ in the system. If there is a NH skin effect, the density at the corresponding edge should be proportional to the system size N, $\rho_{\text{edge}} = \Gamma N$.

This behavior persists in the presence of disorder. For the Hatano-Nelson model, there is only one region of nonzero winding, centered at $E = 0$, so $w(0)$ determines the NH skin effect. In Fig. 4(a,b), we plot the winding $w(0)$ as a function of W_R for (a) $(J_L, J_R, W, W_L) = (1, 1, 0, 0)$ and (b) $(J_L, J_R, W, W_L) = (1, .5, 1, 0)$. This corresponds to the x-axis of Figs. 2(a) and (e). In Fig. 4(c,d) we plot the coefficient Γ for each edge. Any $\Gamma > 0$ indicates a NH skin effect. We see that, identical to the clean case, the NH skin effect occurs at the left edge when $w < 0$ and at the right edge when $w > 0$, and no skin effect occurs when $w = 0$. More intricate models can have regions with both $w > 0$ and $w < 0$, and thus have a skin effect at both boundaries.

The connection between the NH skin effect and $w(E)$ allows us to predict a new phenomenon: the *NH Anderson skin effect*, in which a system without a NH skin effect develops a skin effect at a critical value of disorder.

Such an effect can already be seen in Fig. 2c, in which the system near $(W_L, W_R) = (0, 0)$ has $w(0) = 0$ and thus no NH skin effect, but transitions to $w(0) = \pm 1$ at non-vanishing critical values of W_L or W_R (for example, by tuning one of W_L or W_R and keeping the other zero). Such an effect should be readily observable in experimental platforms[39, 41, 44–46]. This effect is distinct from and independent of the NH topological Anderson insulators explored in Refs. [61, 63], which are NH generalizations of Hermitian topological Anderson insulators. In contrast, the NH Anderson skin effect is unique to NH systems.

As an immediate application, the connection between the NH skin effect and the winding number allows us to understand the stability of the recently demonstrated optical funnel based on the NH skin effect[40]. The optical funnel is a NH optical system in which all eigenmodes are localized at an interface; the effect of this localization is to "funnel" all excitations (incident light) towards the interface. It was noted that for weak disorder numerics show weak funnelling still occurred, while at strong disorder it disappeared. Our formalism allows us to directly predict this phenomena by computing $w(E)$. In the clean limit the entire PBC spectrum surrounds a region with $w(E) \neq 0$, so that all OBC states are localized at the interface. As the disorder increases, the region with $w(E) \neq 0$ shrinks, so that the number of states localized at the interface decreases, leading to reduced funnelling. Finally, at a critical value of disorder, $w(E) = 0$ everywhere and no funnelling occurs. Our formalism not only allows us to understand the stability of the funnelling to weak disorder, but provides a method to compute the critical value of disorder at which funnelling breaks down.

DISCUSSION

We extended the definition of the NH winding number $w(E)$ to disordered systems by relating it to the chiral winding number ν of a doubled Hermitian system. Our extension of $w(E)$ has several desirable properties. It is quantized, self-averaging, continuous as a function of parameters, and changes only when the localization length at E diverges. Additionally, our $w(E)$ successfully predicts the NH skin effect in disordered systems just as it does for clean systems. Unlike Hermitian topological invariants, a nonzero $w(E)$ stabilizes an entire band of delocalized states surrounding the nonzero $w(E)$.

Our prediction of a NH skin effect in strongly disordered systems, including the NH Anderson skin effect, should be experimentally verifiable on existing experimental platforms. In the future, it would be interesting to extend our results to higher dimensions, as the NH skin effect is not fully understood in higher dimensions even for clean systems[41, 90, 91].

ACKNOWLEDGEMENTS

We thank Yuhao Ma for useful discussions. We thank Qi-Bo Zeng for helpful comments on an early version of the manuscript. We thank the US Office of Naval Research (ONR) Multidisciplinary University Research Initiative (MURI) grant N00014-20-1-2325 on Robust Photonic Materials with High-Order Topological Protection for support. We also thank the US National Science Foundation (NSF) Emerging Frontiers in Research and Innovation (EFRI) grant EFMA-1627184 for support. This work made use of the Illinois Campus Cluster, a computing resource that is operated by the Illinois Campus Cluster Program (ICCP) in conjunction with the National Center for Supercomputing Applications (NCSA) and which is supported by funds from the University of Illinois at Urbana-Champaign.

[1] X.-L. Qi and S.-C. Zhang, Topological insulators and superconductors, Rev. Mod. Phys. **83**, 1057 (2011).
[2] M. Z. Hasan and C. L. Kane, Colloquium: topological insulators, Rev. Mod. Phys. **82**, 3045 (2010).
[3] B. A. Bernevig and T. L. Hughes, *Topological insulators and topological superconductors* (Princeton university press, 2013).
[4] A. P. Schnyder, S. Ryu, A. Furusaki, and A. W. W. Ludwig, Classification of topological insulators and superconductors in three spatial dimensions, Phys. Rev. B **78**, 195125 (2008).
[5] X.-L. Qi, T. L. Hughes, and S.-C. Zhang, Topological field theory of time-reversal invariant insulators, Phys. Rev. B **78**, 195424 (2008).
[6] A. Kitaev, Periodic table for topological insulators and superconductors, in *AIP Conference Proceedings*, Vol. 1134 (AIP, 2009) pp. 22–30.
[7] S. Ryu, A. P. Schnyder, A. Furusaki, and A. W. Ludwig, Topological insulators and superconductors: tenfold way and dimensional hierarchy, New J. Phys. **12**, 065010 (2010).
[8] C.-K. Chiu, J. C. Y. Teo, A. P. Schnyder, and S. Ryu, Classification of topological quantum matter with symmetries, Rev. Mod. Phys. **88**, 035005 (2016).
[9] A. Altland and M. R. Zirnbauer, Nonstandard symmetry classes in mesoscopic normal-superconducting hybrid structures, Phys. Rev. B **55**, 1142 (1997).
[10] L. E. F. Torres, Perspective on topological states of non-hermitian lattices, . Phys. Mat. **3**, 014002 (2019).
[11] Y. C. Hu and T. L. Hughes, Absence of topological insulator phases in non-hermitian PT-symmetric hamiltonians, Phys. Rev. B **84**, 153101 (2011).
[12] V. M. Alvarez, J. B. Vargas, M. Berdakin, and L. F. Torres, Topological states of non-hermitian systems, Eur. Phys. J. Spec. Top. **227**, 1295 (2018).
[13] E. J. Bergholtz, J. C. Budich, and F. K. Kunst, Exceptional topology of non-hermitian systems, arXiv preprint arXiv:1912.10048 (2019).
[14] R. El-Ganainy, K. G. Makris, M. Khajavikhan, Z. H. Musslimani, S. Rotter, and D. N. Christodoulides, Non-

hermitian physics and PT symmetry, Nat. Phys. **14**, 11 (2018).
[15] Z. Gong, Y. Ashida, K. Kawabata, K. Takasan, S. Higashikawa, and M. Ueda, Topological phases of non-hermitian systems, Phys. Rev. X **8**, 031079 (2018).
[16] S. Yao and Z. Wang, Edge states and topological invariants of non-hermitian systems, Phys. Rev. Lett. **121**, 086803 (2018).
[17] D. Leykam, K. Y. Bliokh, C. Huang, Y. D. Chong, and F. Nori, Edge modes, degeneracies, and topological numbers in non-hermitian systems, Phys. Rev. Lett. **118**, 040401 (2017).
[18] K. Esaki, M. Sato, K. Hasebe, and M. Kohmoto, Edge states and topological phases in non-hermitian systems, Phys. Rev. B **84**, 205128 (2011).
[19] T. E. Lee, Anomalous edge state in a non-hermitian lattice, Phys. Rev. Lett. **116**, 133903 (2016).
[20] S. Yao, F. Song, and Z. Wang, Non-hermitian chern bands, Phys. Rev. Lett. **121**, 136802 (2018).
[21] S. Lieu, Topological phases in the non-hermitian su-schrieffer-heeger model, Phys. Rev. B **97**, 045106 (2018).
[22] T. Ozawa, H. M. Price, A. Amo, N. Goldman, M. Hafezi, L. Lu, M. C. Rechtsman, D. Schuster, J. Simon, O. Zilberberg, *et al.*, Topological photonics, Rev. Mod. Phys. **91**, 015006 (2019).
[23] S. Weimann, M. Kremer, Y. Plotnik, Y. Lumer, S. Nolte, K. G. Makris, M. Segev, M. C. Rechtsman, and A. Szameit, Topologically protected bound states in photonic parity–time-symmetric crystals, Nat. Mater. **16**, 433 (2017).
[24] G. Harari, M. A. Bandres, Y. Lumer, M. C. Rechtsman, Y. D. Chong, M. Khajavikhan, D. N. Christodoulides, and M. Segev, Topological insulator laser: theory, Science **359**, eaar4003 (2018).
[25] S. Malzard, C. Poli, and H. Schomerus, Topologically protected defect states in open photonic systems with non-hermitian charge-conjugation and parity-time symmetry, Phys. Rev. Lett. **115**, 200402 (2015).
[26] I. Rotter, A non-hermitian hamilton operator and the physics of open quantum systems, J. Phys. A **42**, 153001 (2009).
[27] Y. Xu, S.-T. Wang, and L.-M. Duan, Weyl exceptional rings in a three-dimensional dissipative cold atomic gas, Phys. Rev. Lett. **118**, 045701 (2017).
[28] T. E. Lee and C.-K. Chan, Heralded magnetism in non-hermitian atomic systems, Phys. Rev. X **4**, 041001 (2014).
[29] J. Li, A. K. Harter, J. Liu, L. de Melo, Y. N. Joglekar, and L. Luo, Observation of parity-time symmetry breaking transitions in a dissipative floquet system of ultracold atoms, Nat. Commun. **10**, 1 (2019).
[30] K. Yamamoto, M. Nakagawa, K. Adachi, K. Takasan, M. Ueda, and N. Kawakami, Theory of non-hermitian fermionic superfluidity with a complex-valued interaction, Phys. Rev. Lett. **123**, 123601 (2019).
[31] M. Nakagawa, N. Kawakami, and M. Ueda, Non-hermitian kondo effect in ultracold alkaline-earth atoms, Phys. Rev. Lett. **121**, 203001 (2018).
[32] K. G. Makris, R. El-Ganainy, D. Christodoulides, and Z. H. Musslimani, Beam dynamics in p t symmetric optical lattices, Phys. Rev. Lett. **100**, 103904 (2008).
[33] H. Schomerus, Topologically protected midgap states in complex photonic lattices, Opt. Lett. **38**, 1912 (2013).
[34] L. Xiao, X. Zhan, Z. Bian, K. Wang, X. Zhang, X. Wang, J. Li, K. Mochizuki, D. Kim, N. Kawakami, *et al.*, Observation of topological edge states in parity–time-symmetric quantum walks, Nat. Phys. **13**, 1117 (2017).
[35] B. Zhen, C. W. Hsu, Y. Igarashi, L. Lu, I. Kaminer, A. Pick, S.-L. Chua, J. D. Joannopoulos, and M. Soljačić, Spawning rings of exceptional points out of dirac cones, Nature **525**, 354 (2015).
[36] S. Malzard and H. Schomerus, Bulk and edge-state arcs in non-hermitian coupled-resonator arrays, Phys. Rev. A **98**, 033807 (2018).
[37] A. Cerjan, S. Huang, M. Wang, K. P. Chen, Y. Chong, and M. C. Rechtsman, Experimental realization of a weyl exceptional ring, Nat. Photonics **13**, 623 (2019).
[38] W. Chen, Ş. K. Özdemir, G. Zhao, J. Wiersig, and L. Yang, Exceptional points enhance sensing in an optical microcavity, Nature **548**, 192 (2017).
[39] L. Xiao, T. Deng, K. Wang, G. Zhu, Z. Wang, W. Yi, and P. Xue, Non-hermitian bulk–boundary correspondence in quantum dynamics, Nat. Phys. , 1 (2020).
[40] S. Weidemann, M. Kremer, T. Helbig, T. Hofmann, A. Stegmaier, M. Greiter, R. Thomale, and A. Szameit, Topological funneling of light, Science **368**, 311 (2020).
[41] T. Hofmann, T. Helbig, F. Schindler, N. Salgo, M. Brzezińska, M. Greiter, T. Kiessling, D. Wolf, A. Vollhardt, A. Kabaši, *et al.*, Reciprocal skin effect and its realization in a topolectrical circuit, Phys. Rev. Res. **2**, 023265 (2020).
[42] T. Helbig, T. Hofmann, S. Imhof, M. Abdelghany, T. Kiessling, L. Molenkamp, C. Lee, A. Szameit, M. Greiter, and R. Thomale, Generalized bulk–boundary correspondence in non-hermitian topolectrical circuits, Nat. Phys. , 1 (2020).
[43] H. Jiang, L.-J. Lang, C. Yang, S.-L. Zhu, and S. Chen, Interplay of non-hermitian skin effects and anderson localization in nonreciprocal quasiperiodic lattices, Phys. Rev. B **100**, 054301 (2019).
[44] A. Ghatak, M. Brandenbourger, J. van Wezel, and C. Coulais, Observation of non-hermitian topology and its bulk-edge correspondence, arXiv preprint arXiv:1907.11619 (2019).
[45] M. Brandenbourger, X. Locsin, E. Lerner, and C. Coulais, Non-reciprocal robotic metamaterials, Nat. Commun. **10**, 1 (2019).
[46] D. Zhou and J. Zhang, Non-hermitian topological metamaterials with odd elasticity, Phys. Rev. Res. **2**, 023173 (2020).
[47] H. Schomerus, Nonreciprocal response theory of non-hermitian mechanical metamaterials: Response phase transition from the skin effect of zero modes, Phys. Rev. Res. **2**, 013058 (2020).
[48] C. Scheibner, W. Irvine, and V. Vitelli, Non-hermitian band topology in active and dissipative mechanical metamaterials, arXiv preprint arXiv:2001.04969 (2020).
[49] T. Yoshida and Y. Hatsugai, Exceptional rings protected by emergent symmetry for mechanical systems, Phys. Rev. B **100**, 054109 (2019).
[50] V. Kozii and L. Fu, Non-hermitian topological theory of finite-lifetime quasiparticles: prediction of bulk fermi arc due to exceptional point, arXiv preprint arXiv:1708.05841 (2017).
[51] T. Yoshida, R. Peters, N. Kawakami, and Y. Hatsugai, Symmetry-protected exceptional rings in two-

dimensional correlated systems with chiral symmetry, Phys. Rev. B **99**, 121101(R) (2019).
[52] K. Kawabata, T. Bessho, and M. Sato, Classification of exceptional points and non-hermitian topological semimetals, Phys. Rev. Lett. **123**, 066405 (2019).
[53] J. C. Budich, J. Carlström, F. K. Kunst, and E. J. Bergholtz, Symmetry-protected nodal phases in non-hermitian systems, Phys. Rev. B **99**, 041406(R) (2019).
[54] K. Kawabata, K. Shiozaki, M. Ueda, and M. Sato, Symmetry and topology in non-hermitian physics, Phys. Rev. X **9**, 041015 (2019).
[55] H. Zhou and J. Y. Lee, Periodic table for topological bands with non-hermitian symmetries, Phys. Rev. B **99**, 235112 (2019).
[56] V. M. Alvarez, J. B. Vargas, and L. F. Torres, Non-hermitian robust edge states in one dimension: Anomalous localization and eigenspace condensation at exceptional points, Phys. Rev. B **97**, 121401(R) (2018).
[57] C. H. Lee and R. Thomale, Anatomy of skin modes and topology in non-hermitian systems, Phys. Rev. B **99**, 201103(R) (2019).
[58] Y. Xiong, Why does bulk boundary correspondence fail in some non-hermitian topological models, J. Phys. Commun. **2**, 035043 (2018).
[59] F. K. Kunst, E. Edvardsson, J. C. Budich, and E. J. Bergholtz, Biorthogonal bulk-boundary correspondence in non-hermitian systems, Phys. Rev. Lett. **121**, 026808 (2018).
[60] K. Yokomizo and S. Murakami, Non-bloch band theory of non-hermitian systems, Phys. Rev. Lett. **123**, 066404 (2019).
[61] X.-W. Luo and C. Zhang, Non-hermitian disorder-induced topological insulators, arXiv preprint arXiv:1912.10652 (2019).
[62] F. Song, S. Yao, and Z. Wang, Non-hermitian topological invariants in real space, Phys. Rev. Lett. **123**, 246801 (2019).
[63] D.-W. Zhang, L.-Z. Tang, L.-J. Lang, H. Yan, and S.-L. Zhu, Non-hermitian topological anderson insulators, Sci. China Phys. Mech. **63**, 1 (2020).
[64] L. Jin and Z. Song, Bulk-boundary correspondence in a non-hermitian system in one dimension with chiral inversion symmetry, Phys. Rev. B **99**, 081103(R) (2019).
[65] D. S. Borgnia, A. J. Kruchkov, and R.-J. Slager, Non-hermitian boundary modes and topology, Phys. Rev. Lett. **124**, 056802 (2020).
[66] N. Okuma, K. Kawabata, K. Shiozaki, and M. Sato, Topological origin of non-hermitian skin effects, Phys. Rev. Lett. **124**, 086801 (2020).
[67] K. Zhang, Z. Yang, and C. Fang, Correspondence between winding numbers and skin modes in non-hermitian systems, arXiv preprint arXiv:1910.01131 (2019).
[68] J. Song and E. Prodan, AIII and BDI topological systems at strong disorder, Phys. Rev. B **89**, 224203 (2014).
[69] I. Mondragon-Shem, T. L. Hughes, J. Song, and E. Prodan, Topological criticality in the chiral-symmetric AIII class at strong disorder, Phys. Rev. Lett. **113**, 046802 (2014).
[70] J. Li, R.-L. Chu, J. K. Jain, and S.-Q. Shen, Topological anderson insulator, Phys. Rev. Lett. **102**, 136806 (2009).
[71] C. Groth, M. Wimmer, A. Akhmerov, J. Tworzydło, and C. Beenakker, Theory of the topological anderson insulator, Phys. Rev. Lett. **103**, 196805 (2009).
[72] E. J. Meier, F. A. An, A. Dauphin, M. Maffei, P. Massignan, T. L. Hughes, and B. Gadway, Observation of the topological anderson insulator in disordered atomic wires, Science **362**, 929 (2018).
[73] P. G. Harper, Single band motion of conduction electrons in a uniform magnetic field, Proc. Phys. Soc. A **68**, 874 (1955).
[74] S. Aubry and G. André, Analyticity breaking and anderson localization in incommensurate lattices, Ann. Israel Phys. Soc **3**, 18 (1980).
[75] S. Longhi, Topological phase transition in non-hermitian quasicrystals, Phys. Rev. Lett. **122**, 237601 (2019).
[76] Q.-B. Zeng and Y. Xu, Winding numbers and generalized mobility edges in non-hermitian systems, Phys. Rev. Res. **2**, 033052 (2020).
[77] E. Prodan and H. Schulz-Baldes, Non-commutative odd chern numbers and topological phases of disordered chiral systems, J. Funct. Anal. **271**, 1150 (2016).
[78] E. Prodan and H. Schulz-Baldes, *Bulk and boundary invariants for complex topological insulators*, Mathematical Physics Studies (Springer, 2016).
[79] L. Herviou, J. H. Bardarson, and N. Regnault, Defining a bulk-edge correspondence for non-hermitian hamiltonians via singular-value decomposition, Phys. Rev. A **99**, 052118 (2019).
[80] See Supplemental Material at [URL will be inserted by publisher] for a detailed derivation of our formula for $w(E)$ its properties.
[81] N. Hatano and D. R. Nelson, Localization transitions in non-hermitian quantum mechanics, Phys. Rev. Lett. **77**, 570 (1996).
[82] N. Hatano and D. R. Nelson, Vortex pinning and non-hermitian quantum mechanics, Phys. Rev. B **56**, 8651 (1997).
[83] N. Hatano and D. R. Nelson, Non-hermitian delocalization and eigenfunctions, Phys. Rev. B **58**, 8384 (1998).
[84] J. Pichard and G. Sarma, Finite size scaling approach to anderson localisation, J. Phys. C **14**, L127 (1981).
[85] D. Thouless, A relation between the density of states and range of localization for one dimensional random systems, J. Phys. C **5**, 77 (1972).
[86] I. Y. Goldsheid and B. A. Khoruzhenko, Distribution of eigenvalues in non-hermitian anderson models, Phys. Rev. Lett. **80**, 2897 (1998).
[87] B. I. Halperin, Quantized hall conductance, current-carrying edge states, and the existence of extended states in a two-dimensional disordered potential, Phys. Rev. B **25**, 2185 (1982).
[88] E. Prodan, T. L. Hughes, and B. A. Bernevig, Entanglement spectrum of a disordered topological chern insulator, Phys. Rev. Lett. **105**, 115501 (2010).
[89] M. Onoda, Y. Avishai, and N. Nagaosa, Localization in a quantum spin hall system, Phys. Rev. Lett. **98**, 076802 (2007).
[90] C. H. Lee, L. Li, and J. Gong, Hybrid higher-order skin-topological modes in nonreciprocal systems, Phys. Rev. Lett. **123**, 016805 (2019).
[91] T. Yoshida, T. Mizoguchi, and Y. Hatsugai, Mirror skin effect and its electric circuit simulation, Phys. Rev. Res. **2**, 022062 (2020).